

# High frequency of moraine-dammed lake outburst floods driven by global warming

Received: 14 February 2025

Accepted: 4 December 2025

Published online: 17 December 2025

 Check for updates

Taigang Zhang<sup>1,2</sup>, Weicai Wang<sup>1</sup>✉, Ioannis Kougkoulos<sup>3</sup>, Simon J. Cook<sup>4,5</sup>, Sihan Li<sup>6</sup>, Pablo Iribarren-Anacona<sup>7</sup>, C. Scott Watson<sup>8</sup>, Baosheng An<sup>1</sup> & Tandong Yao<sup>1</sup>

Glacial lake outburst floods (GLOFs) represent a major hazard in mountain regions, yet considerable uncertainty persists regarding whether their frequency has increased in recent decades and to what extent this trend is linked to climate change. Here, we developed a new inventory of GLOFs from moraine-dammed lakes, analyzing 609 events worldwide between 1900 and 2020. Insights from historical reports and geomorphological evidence presented a low but fluctuating increase in the global frequency of reported GLOFs prior to the 1970s. However, a marked acceleration occurred after the 1980s, with the annual frequency increasing from 5.2 GLOFs during 1981–1990 to 15.2 GLOFs during 2011–2020. Overall, the long-term trajectory of reported GLOF frequency closely parallels variations in global air temperature, exhibiting a lag-correlated pattern on timescales of approximately 20 years. The concept of GLOF response time was employed to explain this delayed reaction, which is attributed to warming-induced glacier recession, glacial lake expansion, and slope destabilization surrounding such lakes, ultimately triggering GLOFs.

Glacial lake outburst floods (GLOFs) stemming from moraine-dammed lakes represent a major hazard in mountainous regions<sup>1</sup>. The related cascading processes often span tens to hundreds of kilometers and lead to profound societal and geomorphological consequences<sup>2,3</sup>. For example, in 2023, in the Sikkim Himalaya, the South Lhonak GLOF killed 55 people, with a further 74 reported missing, and caused devastation as far as >160 km downstream, destroying ~30 bridges, 2000 buildings, and three hydropower plants<sup>4,5</sup>. Other catastrophic GLOFs have been well-documented globally, including in British Columbia, Canada<sup>6</sup>, Cordillera Blanca, Peru<sup>7</sup>, and the Patagonian Andes<sup>8,9</sup>, and are garnering increasing scientific and policy interest<sup>10</sup>. The occurrence of GLOFs is typically linked to glacier recession (i.e., debuitressing of valley slopes by shrinking glaciers, and ice avalanches into lakes from unstable ice

fronts), permafrost degradation (rockfalls, landslides, and melting of dead ice in the moraine dam), and extreme weather events (extreme rainfall and melt events), all of which are exacerbated by global warming<sup>11–13</sup>. Nevertheless, the link between GLOFs and climate change remains contentious and is often biased by potential omissions and recording errors<sup>14</sup>. Analysis of existing GLOF inventories has so far shown a decrease or stagnation in frequency at both regional and global scales since the 1980s<sup>15–17</sup>, which seems at odds with the intuitive expectation that, given recent intense warming<sup>18</sup> and glacial lake proliferation<sup>19,20</sup>, GLOF occurrence should have increased.

Constantly updated and revised GLOF inventories are instrumental in addressing these discrepancies. They enable analyses of GLOF frequencies and climate linkages while providing information for

<sup>1</sup>State Key Laboratory of Tibetan Plateau Earth System, Environment and Resources (TPESER), Institute of Tibetan Plateau Research, Chinese Academy of Sciences, Beijing, China. <sup>2</sup>College of Earth and Environmental Sciences, Lanzhou University, Lanzhou, China. <sup>3</sup>Department of Science and Mathematics, Deree –The American College of Greece, Athens, Greece. <sup>4</sup>Division of Energy, Environment and Society, University of Dundee, Dundee, UK. <sup>5</sup>UNESCO Centre for Water Law, Policy and Science, University of Dundee, Dundee, United Kingdom. <sup>6</sup>School of Geography and Planning, University of Sheffield, Sheffield, United Kingdom. <sup>7</sup>Instituto de Ciencias de la Tierra, Facultad de Ciencias, Universidad Austral de Chile, Valdivia, Chile. <sup>8</sup>School of Geography and water@leeds, University of Leeds, Leeds, UK. ✉e-mail: [weicaiwang@itpcas.ac.cn](mailto:weicaiwang@itpcas.ac.cn)

broader applications, such as validating the reliability of GLOF susceptibility assessments<sup>21</sup>, identifying lakes for GLOF scenario modeling<sup>22–24</sup>, and informing GLOF risk mitigation and policy development<sup>25,26</sup>. A precise GLOF chronology can be constructed using two approaches. The first involves compiling events reported in documented sources, including journal papers, news reports, and local administrative records<sup>27</sup>. The second integrates post-failure geomorphic analysis, leveraging GLOF traces such as decreases in lake levels, breached dams, outwash fans, and downstream devastation, to identify previously unreported events<sup>28,29</sup>. Employing manual or computer-automated analysis of images from diverse sources can substantially enrich inventories. Research in the Himalaya<sup>17</sup>, tropical Andes<sup>7</sup>, and Southern Andes<sup>30</sup> indicates that relying solely on passively reported information underestimates the quantity of moraine-dammed GLOFs by 0.5–2 times. Thus, constructing a global GLOF inventory necessitates continuous updating of reported events, as well as proactive identification of unreported historic GLOFs via geomorphic assessments. Moreover, for ambiguous cases, GLOF traces can confirm their reliability<sup>31</sup>, while extensive satellite imagery archives such as Landsat and Sentinel can be used to further constrain GLOF timing for those events with otherwise large time-of-outburst windows. The latest global inventory (version 4.1) includes 463 moraine-dammed GLOFs that occurred between 1900 and 2020<sup>32</sup> but still requires improvements in completeness, continuity, and accuracy.

In this work, we present an updated global inventory of moraine-dammed GLOFs that enables systematic analysis of their distributions, frequencies, and climatic connections. We apply a three-step framework consisting of dataset synthesis, outburst timing calibration, and

identification of unreported GLOFs (see Methods) to improve the dataset quality and support robust assessments of GLOF characteristics across different spatiotemporal scales. Key findings indicate a phased increase in GLOF frequency since the 20th century, largely driven by intensified global warming.

## Results

### GLOF distribution and frequency

By synthesizing diverse regional inventories and conducting systematic geomorphic assessments, we identified an additional 178 GLOFs from documented sources and detected an additional 88 GLOFs, which were incorporated into the latest global inventory. The reliability of each GLOF was validated by assessing residual geomorphic traces in satellite imagery. In total, these efforts led to the compilation of 609 GLOFs that originated from 512 different moraine-dammed lakes globally during 1900–2020 (Fig. 1a). This represents a 285% increase compared to the first dedicated GLOF inventory published in 2018<sup>16</sup> and a 32% increase compared to the latest version published in 2024<sup>32</sup>.

The GLOFs were mainly concentrated in the Third Pole (encompassing Central Asia, South Asia West, and South Asia East; 241 GLOFs, accounting for 39.6% of the total), the Low Latitudes (132, 21.7%), the Southern Andes (96, 15.8%), western Canada and the USA (52, 8.5%), Central Europe (26, 4.3%), and Svalbard (23, 3.8%). At the national level, moraine-dammed GLOFs originated in 26 countries or autonomous regions. Peru, China, and Chile were the most affected countries, with 117, 112, and 74 GLOFs, respectively. Although failed moraine-dammed lakes accounted for only 0.8% of the global total number of such lakes<sup>20</sup>, this proportion is highly heterogeneous across glaciated

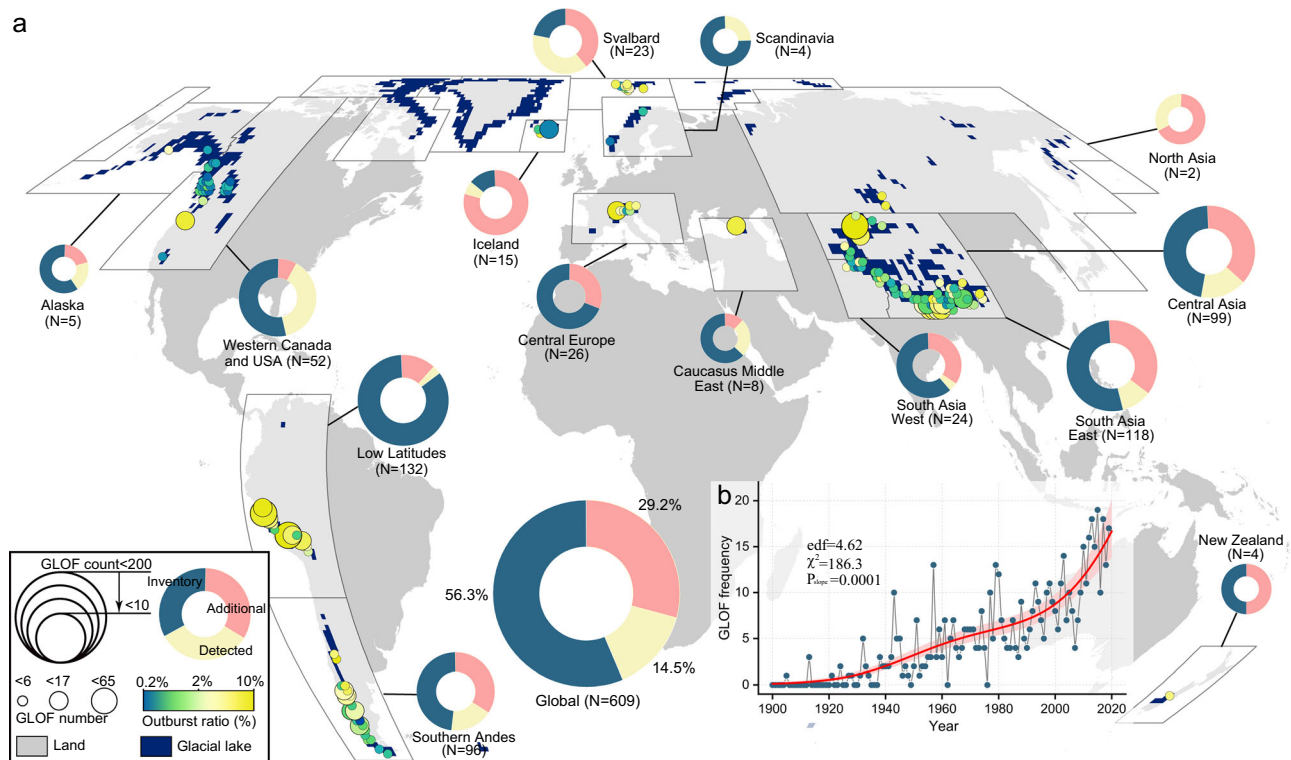


**Fig. 1 | Revised global inventory of moraine-dammed GLOFs and their spatial distribution.** **a** The maps show the global distribution, local number, and relative densities of GLOFs during 1900–2020. The circles are scaled according to the number of GLOFs within each  $1^\circ \times 1^\circ$  tile and are color-coded to indicate the proportion of locally drained lakes relative to the total. The pie charts aggregate the regional GLOF count based on the Global Terrestrial Network for Glaciers (GTN-G) regions, and display their respective data sources, including the latest global inventory v4.0 (*Inventory*), supplementary data from other reports (*Additional*),

and the newly detected events identified via geomorphic assessments in this study (*Detected*). The distribution data for glacial lakes in 2020 is sourced from Zhang et al.<sup>20</sup>. **b** A linear fit for annual GLOF frequency was performed using the generalized additive model. The degrees of freedom (edf) and chi-square statistic ( $\chi^2$ ) indicate the complexity and goodness of fit, with lower values suggesting a better model. The  $p$ -value for the mean slope ( $P_{\text{slope}}$ ) reflects the significance of the trend. Map source: Natural Earth (public domain).

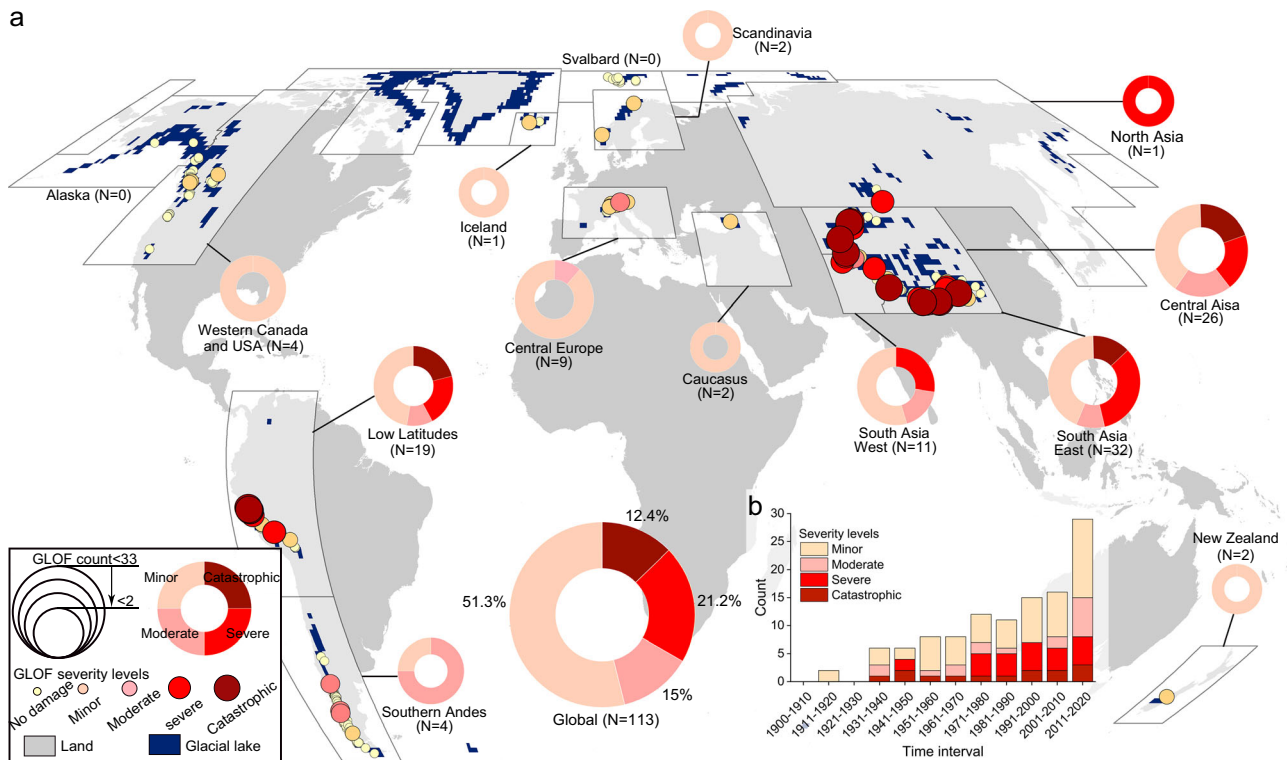


**Fig. 2 | Occurrence of destructive GLOFs worldwide since 1900. a** Based on documented downstream damage, the GLOFs were classified into different levels of severity. The GLOFs without impact reports were categorized as no damage, while the other destructive GLOFs were further classified into minor, moderate, severe,

and catastrophic categories. The pie charts summarize the regional GLOF counts with reported damage, grouped according to the GTN-G regions. **b** The temporal trends of the frequency of destructive GLOFs are presented in ten-year intervals. Map source: Natural Earth (public domain).

regions. The outburst ratios were 6.3% in the Low Latitudes, 3.7% in Central Europe, 1.7% in the Third Pole, 1.6% in the Southern Andes, and 1.1% in Svalbard, while western Canada and the USA had a relatively lower ratio of 0.5%.

Globally, moraine-dammed GLOF frequency showed a fluctuating increase between 1900 and 2020 (Fig. 1b). Three distinct transition epochs were identified: (i) prior to the late 1930s, GLOFs were rarely reported worldwide; (ii) from the early 1940s to late 1970s, reporting frequency increased gradually, with a mean of 4.5 GLOFs per year, consistent with previous findings<sup>16</sup>; and (iii) after the 1980s, GLOF reporting entered a phase of acceleration, increasing from an average of 5.2 GLOFs per year during 1981–1990 to 15.2 GLOFs per year during 2011–2020.

### GLOF impacts and downstream damage

A total of 113 (18.6%) moraine-dammed GLOFs had recorded downstream damage (Fig. 2a), including fatalities and impacts on bridges, roads, farmland, forests, and hydropower projects. Since 1900, these events have collectively caused over 13,000 fatalities worldwide. Among the most catastrophic were the 1941 Palcacocha GLOF in Peru<sup>33</sup> and the 2013 Chorabari GLOF<sup>34</sup> in India, both of which devastated downstream settlements and claimed thousands of lives. To quantify impacts, we categorized descriptive damage reports into five levels, ranging from no damage to catastrophic. This categorization accounts for the extent of losses to infrastructure and communities, albeit with some subjectivity. Spatially, the Third Pole and the Low Latitudes were the most affected regions, encompassing 37 severe and catastrophic GLOFs. This also means that most of the recorded casualties and major infrastructure losses were concentrated there. Temporally, of the 65 GLOFs that occurred in the 1970s, twelve caused recorded damage (accounting for 18% of the events). This number increased to 33 out of 151 GLOFs in the 2010s (22%), reflecting increases in both the number

and proportion of GLOFs with disastrous societal impacts (Fig. 2b). Furthermore, we mapped the loss in lake area for 362 GLOFs since the 1980s using satellite imagery. Notably, complete drainage was observed in 20% of these cases. Our analysis found no significant correlation between GLOF severity and lake size (Supplementary Fig. S1). GLOFs originating from medium/large lakes (>0.1 km<sup>2</sup>) were not necessarily associated with severe disasters, as their impacts depended jointly on drainage volume and downstream exposure. Likewise, GLOFs originating from small lakes were not always harmless<sup>35,36</sup>; that is, 18 events were characterized by small outbursts but large disasters.

## Discussion

### Warming effects on GLOF activity

To explore potential connections between climate change and GLOF activity, we combined temperature and precipitation records from the Climate Research Unit (CRU) dataset with data on glacial lake expansion and concomitant GLOF triggers across multiple spatiotemporal scales. The analysis showed a lag-correlated temporal pattern between global temperature and reported GLOF frequency. There is a consensus that global temperatures entered a sustained warming phase after the 1970s<sup>18</sup>, coinciding with the sharp rise in GLOF frequency over the past four decades (Supplementary Fig. S2). Before the 1970s, temperatures fluctuated, mirroring the relatively low and gradual increase in GLOF frequency. The influence of temperature intensifies with increasing spatial scale, from local to global (Fig. 3a). Consistent lagged responses of 0–5 and 10–14 years are evident, and there is a credible -20 years lag between warming effects and GLOF occurrence at the global scale ( $r > 0.5$ ,  $P < 0.01$ ). By contrast, precipitation does not exhibit a consistent or statistically significant influence on interannual variations in GLOF frequency (Fig. 3b).

The concept of GLOF response time is essential for interpreting these lags, reflecting the combined timelines of glacier recession,

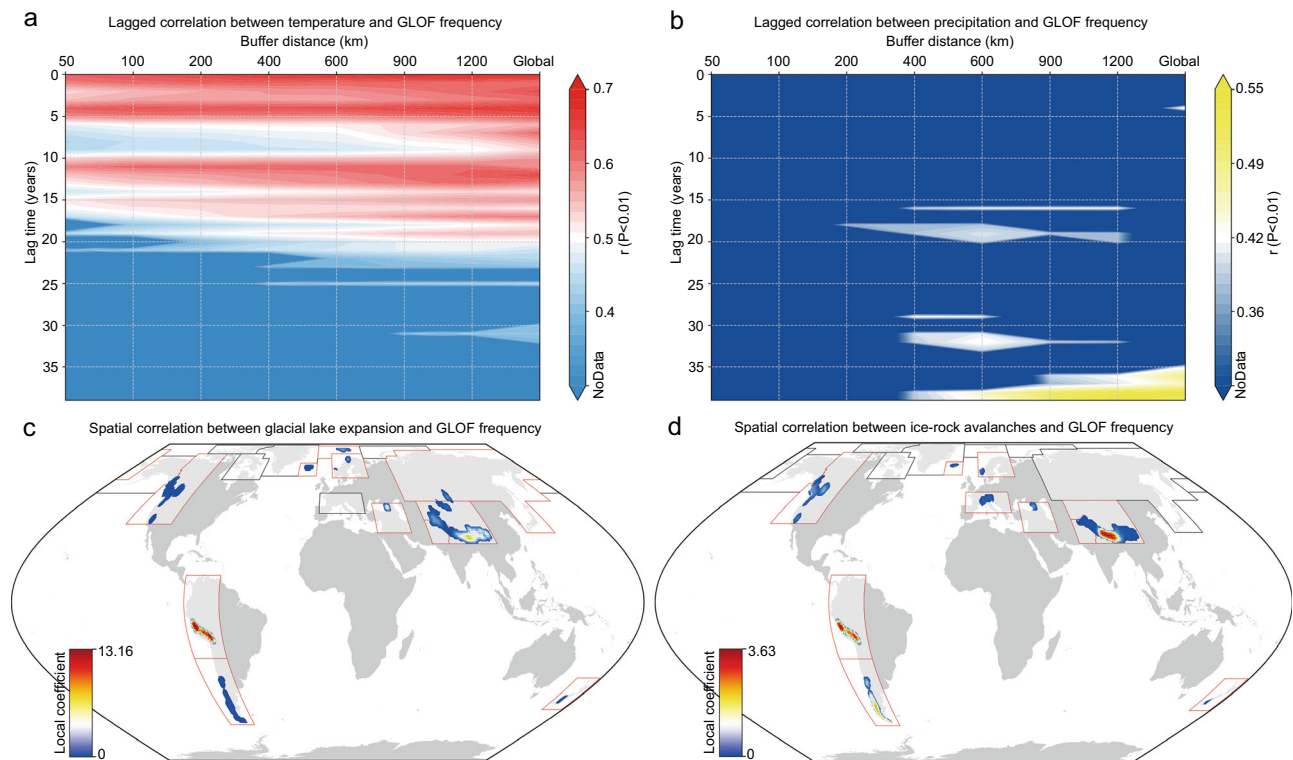


**Fig. 3 | Connections between climatic factors, response timelines, and GLOF activity.** **a, b** Correlations between global GLOF frequency during 1940–2020 and interannual variations in temperature and precipitation at multiple spatial scales and lag intervals. **c, d** Spatial relationships between regional GLOF activity and glacial lake expansion (1990–2020), as well as ice-rock avalanches (1900–2019), derived using a Geographically Weighted Regression (GWR) model. Local

coefficients indicate the extent of the positive influence to which lake expansion or avalanches contribute to GLOF activity at each observation point. For instance, a local coefficient of 1.5 signifies that, in a given area, a one-unit increase in the explanatory variable corresponds to a 1.5-fold increase in GLOF activity. Map source: Natural Earth (public domain).

glacial lake expansion, and the development of triggering conditions<sup>16,37,38</sup>. Our spatial correlation analysis further showed that, with the exception of Central Europe and Svalbard, all major GLOF regions exhibit positive connections between GLOF activity, glacial lake expansion, and ice-rock avalanches. The strongest linkages are found in the Southern Andes, Low Latitudes, and Himalaya (Fig. 3c, d). Ice avalanches and rockfalls or landslides are the dominant triggers, accounting for ~70% of outbursts in the Third Pole, Low Latitudes, and Southern Andes<sup>21,30,39</sup>. The stability of glaciers and frozen slopes is highly sensitive to climate change. Rising temperatures drive a thermal shift from cold-based to polythermal or temperate glaciers, altering the frequency and magnitude of ice avalanches<sup>40,41</sup>. Similarly, slopes surrounding glacial lakes become increasingly susceptible to failure under shifts in precipitation phase and repeated freeze–thaw cycles<sup>42–45</sup>. For example, the 2020 Elliot Creek GLOF in British Columbia, Canada, was triggered by an  $18 \times 10^6 \text{ m}^3$  landslide from a degrading lateral slope<sup>46</sup>. Indeed, these warming-induced shifts in the thermal dynamics of ice/rock materials inherently produce lagged effects. Stoffel et al.<sup>47</sup> reconstructed rockfall ( $<10^3 \text{ m}^3$ ) rates from a thawing slope in the Swiss Alps and found a significant temperature correlation with delayed reaction. Globally, ice and rock avalanche frequency also demonstrated a lag of 10–20 years to temperature variations<sup>48</sup>. Beyond this, another physical manifestation of this lag-time concept lies in the longevity of most glacial lakes prior to their outbursts. Analysis of 388 post-1981 GLOFs from the updated inventory showed that 96.3% of failed lakes had existed for more than 5 years, 87.6% for over 10 years, and 60.1% for over 20 years before failure (Supplementary Table S1).

Collectively, lake expansion arising directly from widespread glacier recession under warming<sup>20</sup>, coupled with the maturation and occurrence of triggers, governs GLOF response time. Within this

process chain, glacier recession and glacial lake expansion proceed synchronously, as do triggering events and resultant GLOFs, both producing immediate impacts and without appreciable delays between them. The observed temporal lag thus arises mainly from the time required for lake expansion and slope destabilization under sustained warming. We surmise that GLOFs are initiated when these two processes intersect; otherwise, the lakes remain unbreached. This mechanism explains why the observed GLOF response time approximates both the lag reported for avalanches and the longevity of the failed lakes, providing evidence that global warming drives GLOF activity.

### Regional GLOF patterns and trend

The six regions in Fig. 4 with the greatest GLOF activity have experienced substantial glacier ice loss (with a mass balance of  $-0.6$  to  $-1.3 \text{ m.w.e.a}^{-1}$ )<sup>49,50</sup> and glacial lake expansion with areal increase of 6–30%<sup>9,20,51–53</sup> in recent decades. Despite the marked increase in the frequency of reported GLOFs globally after the 1980s, their occurrence is affected not only by warming-induced process chains but also by regional topography and human activities, leading to considerable spatial heterogeneity. Our statistical analysis revealed that, since 1981, the reported GLOF frequency has increased in the Third Pole, the Low Latitudes, Svalbard, and the Southern Andes ( $P < 0.05$ ); remained stable in western Canada and the USA; and decreased in Central Europe. When moraine-dammed lakes are situated in broad, low-gradient glaciated valleys, the influence of surrounding slopes and glaciers is greatly diminished<sup>54</sup>. This is most evident in Alaska, where glacial lakes have expanded the fastest globally, yet only five GLOFs have been reported<sup>55</sup>. An analogous pattern was also observed in neighboring western Canada and the USA. In Central Europe, most GLOFs were reported prior to 2000, with only one event recorded after 2010<sup>56</sup>. A possible reason for this trend is extensive human

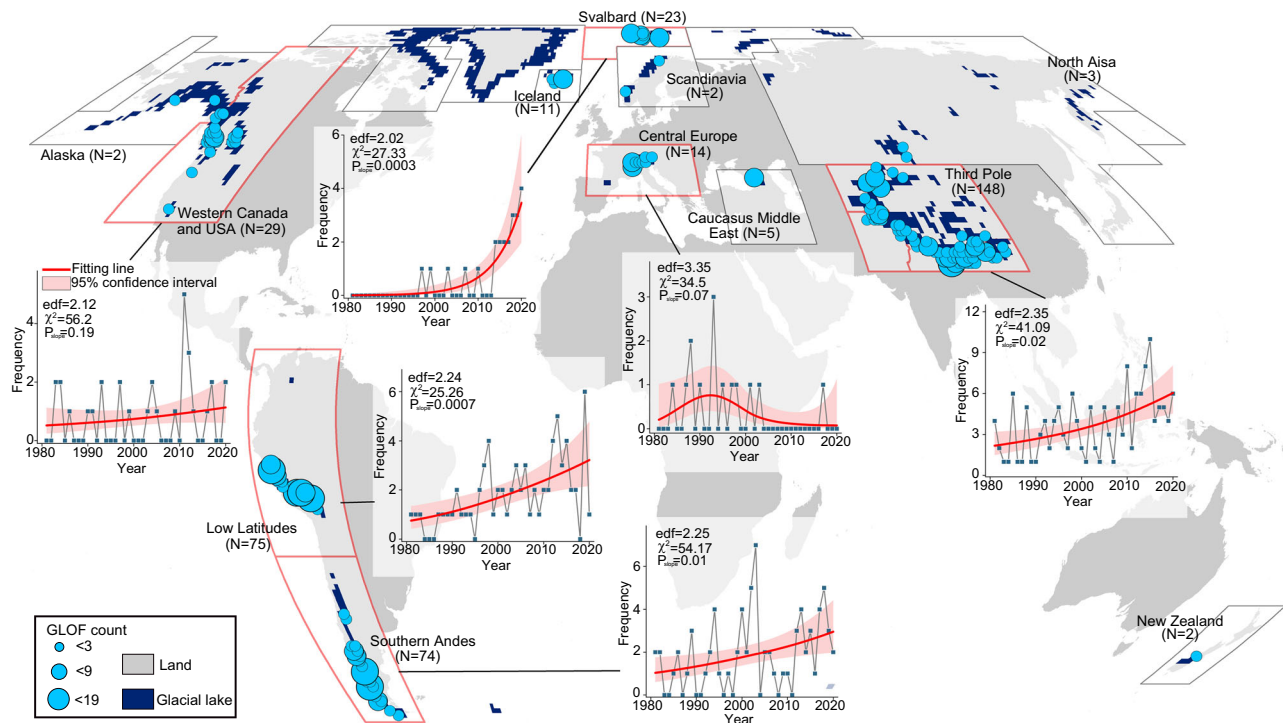


**Fig. 4 | Regional GLOF trends since 1981.** The maps illustrate the distribution of GLOFs following the fitted trends of annual GLOF frequency in glaciated regions. The circles were scaled according to the number of GLOFs within each  $1^\circ \times 1^\circ$  tile. The associated annual GLOF frequencies during 1981–2020 were aggregated and

fitted using the generalized additive model to reveal their temporal trends. This period coincides with the satellite era and heightened research interest, yielding relatively extensive reporting rates for GLOFs. Map source: Natural Earth (public domain).

interventions in this region, including the construction of alpine hydro-power plants, managed lake drainage, and moraine dam reinforcements, which have effectively restricted lake development and mitigated the risks associated with mass movements<sup>54,57</sup>.

By synthesizing historical reports and geomorphological evidence, this study compiled a global inventory of 609 moraine-dammed GLOFs between 1900 and 2020. Both a marked global acceleration of GLOFs since the 1980s and pronounced regional heterogeneity were revealed. These patterns are driven not only by warming-induced process chains but also strongly modulated by regional topography and human activity, collectively shaping the spatiotemporal distribution of GLOFs. Debates persist regarding whether or not GLOF frequency has increased globally or regionally over recent decades. Harrison et al.<sup>16</sup> reported a decline in GLOF frequency after the 1970s based on the first global moraine-dammed GLOF inventory, while Veh et al.<sup>17</sup> found stable frequency in the Himalaya after the 1980s. Similar conclusions were drawn by several other studies<sup>14,15,32</sup> (Supplementary Fig. S3). We suggest that the discrepancy in findings about GLOF frequency in our study compared to these previous studies may be explained by three factors: (i) Misclassification of events: many earlier inventories included erroneous reports, leading to inflated GLOF counts during specific periods and thereby distorting trend analyses. For instance, glacial debris flows or ice/rock avalanches, which can cause similar channel erosion and infrastructure damage, were often misclassified as GLOFs. Nie et al.<sup>31</sup> suggested that approximately one-sixth of reported GLOFs may be unreliable in the Himalaya. (ii) Conflation of lake types: ice-dammed and supraglacial lakes are capable of producing GLOFs, yet their outburst mechanisms differ from those of moraine-dammed lakes. For instance, ice-dammed GLOFs are typically triggered by flotation or collapse of the ice dam, or the formation of subglacial channels, involving distinct process chains. Failure to distinguish these GLOF types will potentially distort trend analysis. (iii) Database construction

limitations: most GLOF inventories have been built based on documented sources, leading to underreporting of events. Without continuous updates, such biases will be uncontrolled in records.

### Updated GLOF inventory and risk implications

Revealing GLOF trends and their potential drivers depends on a reliable inventory, yet achieving such reliability remains challenging. Beyond unknown historical underreporting, geomorphic assessment is constrained by image resolution, cloud cover, and satellite acquisition rate, as well as the rapid concealment of GLOF traces through vegetation succession, human interventions (i.e., dam immobilization and mining), and geomorphic remodeling (fluvial erosion and meander shifts)<sup>38</sup>. To glimpse potential biases in reporting and detection rates, we examined the structural properties of the revised database. Two lines of evidence suggest that it provides a robust basis for statistical analyses. First, pre-failure lake areas exhibit a power-law distribution (Supplementary Fig. S4). This accords with physical reasoning, as under the assumption that those triggering events such as ice avalanches and landslides occur without spatial bias at the regional scale, smaller lakes are more numerous and thus statistically more likely to encounter such triggers. Hence, the intrinsic area distribution of glacial lakes largely governs the size of failed lakes, with smaller ones failing more frequently than larger ones<sup>59</sup>. Second, GLOF frequency trends are consistent across size classes ( $r > 0.86$ ) (Supplementary Fig. S5), such as the tested intervals ( $\text{km}^2$ ) S1: [0.02, 0.06], S2: [0.06, 0.16], and S3: [0.16, 2.0]. This indicates scale invariance with separable temporal effects<sup>60</sup>, as the frequencies of GLOFs in different pre-failure size classes exhibit a stable proportional relationship. Together, these features indicate no significant bias toward specific lake-size intervals within the study period, suggesting an internally consistent database structure. Certainly, because the inventory is still constructed based on passive factual records, it should be regarded as a lower bound for all trend analyses relative to the actual situation.

GLOFs are a prominent geomorphic process within the cryosphere, and their intersections with social and environmental factors have caused catastrophic damage. This study quantifies global and regional GLOF frequency and their societal impacts, while emphasizing the role of glaciers, glacial lakes, and trigger events under global warming in attribution analyses. The updated and revised inventory will facilitate regional GLOF risk assessments, disaster prevention and mitigation, and policy formulation. Recently, the heightened research focus on GLOFs mainly reflects their catastrophic consequence, which is difficult to predict and prevent, posing challenges to local sustainable development in alpine regions<sup>61</sup>. Societal impacts of GLOFs are staggering in the Cordillera Blanca and the Third Pole. Regarding the dynamics between society and cryospheric hazards, the core of risk management lies in reducing exposure and vulnerability while enhancing resilience<sup>62</sup>. Adaptation in mountainous regions can currently be divided into three levels<sup>57</sup>. The first level involves deepening the understanding of disaster characteristics, including field investigations, database construction, and risk assessment. The second level involves structural measures to prevent or effectively mitigate natural hazards<sup>26,63</sup>. Common remedial works include early warning systems, artificial lake drainage, and dam reinforcement. The third level is systematic, focusing on holistic risk management through non-structural measures such as policy development, public awareness initiatives, and strengthening the resilience of socio-economic systems. Under future scenarios of sustained warming<sup>64–67</sup>, the intensification of GLOF activity seems inevitable. Comprehensive, site-specific assessments that integrate climatic, topographic, and anthropogenic drivers are urgently needed to elucidate the mechanisms governing GLOF occurrence<sup>38</sup>. Meanwhile, strengthening scientific understanding, engineering measures, and risk management will be crucial to improve adaptive capacity to GLOF hazards. In the near future, representative platforms should be established to facilitate collaboration and communication on GLOFs<sup>68</sup>, raising awareness among governments and local communities of the increasing disaster risks driven by climate change.

## Methods

### Tracking moraine-dammed GLOFs

Moraine-dammed lakes have experienced extensive and frequent outbursts in recent decades<sup>69</sup>. Here, we specifically examined global moraine-dammed GLOFs that occurred between 1900 and 2020 to establish a robust inventory, which could then be used to analyze GLOF characteristics. Omissions and recording errors significantly affect the quality of inventories and the reliability of subsequent analyses. These issues stem in part from regionality challenges in GLOF research, as well as from limited database cross-checking and geomorphic assessment. To bridge these gaps, three key efforts were undertaken to develop a robust inventory: dataset synthesis, outburst timing calibration, and detection of previously unreported GLOFs.

First, the latest global GLOF inventory (version 4.0)<sup>32</sup> was used as a benchmark dataset that we supplemented with other regional inventories and sporadically reported events. A total of 463 GLOFs during 1900–2020 were extracted from the global inventory<sup>32</sup>; their locations were traced using Google Earth. Additionally, we reviewed the first-hand descriptions for each GLOF from the literature source where they were first reported. Residual GLOF traces<sup>58</sup>, including decreases in lake levels, breached dams, outwash fans, and downstream devastation were further validated based on imagery archives of the Key Hole (KH) (between the 1960s and 1984) and Landsat (since the 1980s) satellites. Consequently, 120 GLOFs were excluded due to missing location, duplicate records, or insufficient geomorphic evidence (Supplementary Table S2). Most of these unconvincing reports emerged in the northern Tien Shan, where the drained lakes had very small pre-failure areas (generally <0.005 km<sup>2</sup>) or lacked evident damming features, characterizing a distinctive pattern of repeated outburst. For example, the Aksay Glacier alone accounted for 25 GLOFs during the study

period. Similar behavior was observed in 11 other counterparts, resulting in a total of 93 GLOFs (Supplementary Fig. S6). This finding is counterintuitive, as outbursts of moraine-dammed lakes are generally non-repeating events unless the dam is only partially breached. Review of original literature revealed that many GLOFs in this region were described using qualifiers such as “very likely” or “likely”<sup>70,71</sup>. Based on geomorphic evidence and the firsthand descriptions, some of these reports likely correspond to glacial debris flows or drainages from supraglacial or subglacial lakes. Other contributions and omissions from our revised GLOF reports include the following:

- (i) Shrestha et al.<sup>72</sup> reported 331 moraine-dammed GLOFs in the Third Pole during 1900–2020. Upon screening, 62 of these events were not recorded in the global inventory, and 122 GLOFs were deemed unreliable after assessment. Most of the excluded GLOFs came either from preliminary geomorphic analyses by Zheng et al.<sup>73</sup> or from the northern Tien Shan. Lack of geomorphic evidence was defined as two specific criteria: traces existed before the lake formed, or the lake existed but no definitive GLOF traces (Supplementary Fig. S7). Geomorphic validations were conducted cautiously, ensuring that each exclusion was well justified.
- (ii) In the tropical Andes, Emmer et al.<sup>7</sup> conducted a systematic geomorphic assessment and review of documentary data, increasing the GLOF count from 53 to 160. Similarly, in the Patagonian Andes, Colavitto et al.<sup>30</sup> applied the same method to increase the GLOF count from 36 to 71. All validated moraine-dammed GLOFs were incorporated into our revised inventory.
- (iii) In Svalbard, Wiczorek et al.<sup>74</sup> reported some GLOFs, but no public data were available. Hence, we conducted our own search in the region and included 9 events into the inventory. Those events that did not originate from moraine-dammed lakes or were merely due to periodic meltwater inflow/outflow causing areal changes, were excluded. Additionally, some previously overlooked sporadic reports, such as the 2002 Dasht GLOF in Pamir<sup>75</sup> and the 2018 Zalai Tsho GLOF in Nyainqentanglha<sup>76</sup>, were also incorporated. In total, dataset synthesis added 178 GLOFs into the latest global inventory (Supplementary Fig. S8 and Supplementary Table S3).

Second, we constrained outburst timing to address imprecise temporal records. A total of 256 GLOFs were labeled with broad time-of-outburst window or “before-year” designations. By utilizing time-series satellite imagery from KH and Landsat, we calibrated these GLOFs and reduced the average timing uncertainty to 3.4 years. For frequency analysis, GLOFs with defined windows were assigned the outburst timing as the midpoint, whereas “before-year” events were assigned a date five years prior to the indicated year. This ensured that each GLOF had a specific failure date.

Third, previously unreported GLOFs were detected through systematic geomorphic assessments according to the methodology outlined by Emmer et al.<sup>7</sup>. Dam breaches and lake level decreases are typically preserved on centennial scales, while outwash fans and downstream devastation can be obscured over several decades<sup>58</sup>. Using these four key indicators, a holistic assessment and manual supervision were conducted across all glaciated regions (Supplementary Fig. S9). Likely GLOF traces were first identified on Google Earth, after which 1255 Sentinel-2A/B images acquired in 2020 were further analyzed to detect and validate residual traces. This process led to the discovery of 88 new GLOFs worldwide (Supplementary Fig. S10 and Supplementary Table S4).

### Classification of destructive GLOFs

Within the revised inventory, 287 GLOFs were collected from documentary sources, and 322 were detected via geomorphic assessments conducted as part of the present study as well as from other earlier

studies<sup>17,30,73</sup>. A study in the Himalaya revealed that the newly detected GLOFs tended to have shorter runout distances or occurred in areas with lower population densities<sup>17</sup>. In contrast, documented events are more likely to be associated with damage records and long-lasting geomorphic impacts. To standardize reporting, GLOFs were categorized into five different severity levels based on reported losses. Events with no reported impacts on downstream infrastructure and communities were classified as no damage, while the minor and moderate levels were determined by the extent of infrastructure damage and economic impact. The severe and catastrophic levels were characterized by tragic consequences, as indicated by the number of fatalities and serious infrastructure losses such as hydropower plants (Supplementary Table S5). Of the 113 GLOFs with recorded damage in our inventory, 99 were derived from literature reports, including most of the moderate, severe, and catastrophic cases. Additionally, to further uncover links between GLOF severities and lake features, the pre- and post-failure lake areas were manually delineated using satellite imagery. For the GLOFs that occurred prior to the satellite era, their areas were estimated based on early glacier extents and the lake accommodation potential (Supplementary Fig. S11). A total of 41 declassified Corona KH-4 and 27 Hexagon KH-9, and 281 Landsat 4/5 TM, 74 Landsat 7 ETM+, and 158 Landsat 8 OLI TIRS images were utilized in this process, as well as the prior GLOF trace validation and outburst timing calibration.

### Driving factors of GLOFs

The connections between climate change, response timelines, and GLOF activity were described quantitatively. First, annual mean 2-m temperature and precipitation records were extracted from the Climate Research Unit time-series version 4.05 (CRU TS v4.05)<sup>77</sup> within different buffer ranges (50, 100, 200, 400, 600, 900, and 1200 km, as well as the global scale) around each of the GLOF locations within our revised inventory, between 1900 and 2020. This enabled an evaluation of possible climatic influences on GLOF activity across different spatial scales. Meanwhile, to assess the potential for any delays between climate forcing and of GLOF incidence, the strength of correlations was calculated between global GLOF frequency from 1940 to 2020 and temperature/precipitation lagged by 0–39 years (i.e., from 1940–2020 to 1901–1981). We retained only those instances where the Pearson's correlation coefficient ( $r$ ) met the significance threshold of  $P < 0.01$  in order to highlight only the most robust relationships. Notably, 16 GLOFs explicitly triggered by earthquakes or glacier surges were excluded to focus on GLOFs that could potentially have been promoted by climate change-related factors<sup>78</sup>.

Second, a Geographically Weighted Regression (GWR) model was used to explore spatially varying relationship between GLOF activity and potential driving factors. GWR accounts for local spatial heterogeneity by allowing regression coefficients to vary across geographic space. It can be expressed as:

$$y_i = \beta_0(u_i, v_i) + \beta_1(u_i, v_i) \cdot x_i + \varepsilon_i \quad (1)$$

where  $y_i$  is the dependent variable (GLOF frequency) at location  $i$ ;  $x_i$  is the independent variable (including glacial lake expansion rate and ice-rock avalanches frequency);  $\beta_1$  is the location-specific coefficient at coordinates  $(u_i, v_i)$ ;  $\varepsilon_i$  is the error term.

Two key driving factors were considered: (i) the glacial lake expansion rate ( $\text{km}^2/5\text{a}$ ) during 1990–2020, derived from the latest global glacial lake inventory<sup>20</sup>, representing a long-term preparatory factor; and (ii) the frequency of ice-rock avalanches during 1900–2019, compiled from historical disaster archives<sup>48</sup>, serving as a representative triggering factor. Together with the dependent variable of GLOF activity, all data were aggregated to  $1^\circ \times 1^\circ$  tiles on consistent time-scales. GWR was implemented in ArcGIS software with an adaptive Gaussian kernel, and the optimal bandwidth was determined by the

corrected Akaike Information Criterion. Model performance was evaluated via  $R^2$ , residual diagnostics, and comparison with a global Ordinary Least Squares regression model. The outputs consist of spatially explicit local coefficients, reflecting the impact of lake expansion or ice and rock avalanches on GLOF activity across different glaciated regions.

### Temporal trends of GLOFs

A generalized additive model (GAM), which is a nonparametric regression technique<sup>79</sup>, was employed to evaluate the temporal trends in GLOF frequency. This model decomposes the nonlinear effects of the predictor variables into a sum of smooth functions, allowing it to capture complex nonlinear relationships. The basic structure of the GAM is expressed by the following equation:

$$g(\mu) = \alpha + \sum_{j=1}^p f_j(X_j), \quad (2)$$

where  $g(\mu)$  is the link function,  $\alpha$  is the intercept term, and  $f_j(X_j)$  is the smooth function of the predictor  $X_j$ . Here,  $f_j$  is specified using basis functions such as splines, allowing the effect of each predictor to vary nonlinearly, and  $X_j$  denotes the  $j$ -th explanatory variable included in the model.

In this study, the PoissonGAM was selected as the fitting model, which is appropriate for modeling count data with the year as the predictor variable<sup>80</sup>. The model utilized quadratic spline functions for smoothing, and cross-validation and the Akaike information criterion was used to assess the model performance. To further evaluate the model's significance, the estimated slopes of each smooth function and the associated  $p$ -values of the fitted trends were calculated. Additionally, the estimated degrees of freedom (edf) were calculated to reflect the model's complexity and smoothness, and the chi-squared ( $\chi^2$ ) statistic was used to assess the goodness of fit.

### Data availability

The Landsat and KH images can be downloaded from the United States Geological Survey (USGS) at <https://earthexplorer.usgs.gov/>. The Sentinel images can be downloaded at <https://dataspace.copernicus.eu/>. The CRU TS dataset can be downloaded at <https://crudata.uea.ac.uk/cru/data/hrg/>. The version-controlled inventory of global glacial lake outburst floods can be downloaded at <http://glofs.geoecology.uni-potsdam.de/>. The latest inventory of ice and rock avalanches inventory can be downloaded at <https://doi.org/10.11888/Cryos.tpd.272812>. The inventory of global glacial lakes in 1990 and 2020 can be downloaded from the National Tibetan Plateau/Third Pole Environment Data Center at <https://doi.org/10.11888/Cryos.tpd.300938>. Our revised global-scale GLOF inventory can be downloaded at <https://doi.org/10.5281/zenodo.14643434>.

### Code availability

Code for the trend analysis of PoissonGAM is available at <https://github.com/Taigang1/GLOF>.

### References

- Richardson, S. D. & Reynolds, J. M. An overview of glacial hazards in the Himalayas. *Quat. Int.* **65**, 31–47 (2000).
- Carrivick, J. L. & Tweed, F. S. Proglacial lakes: character, behaviour and geological importance. *Quat. Sci. Rev.* **78**, 34–52 (2013).
- Cook, K. L., Andermann, C., Gimbert, F., Adhikari, B. R. & Hovius, N. Glacial lake outburst floods as drivers of fluvial erosion in the Himalaya. *Science* **362**, 53–57 (2018).
- Zhang, T., Wang, W. & An, B. A massive lateral moraine collapse triggered the 2023 South Lhonak Lake outburst flood, Sikkim Himalayas. *Landslides* **21**, 1–13 (2024).

5. Sattar, A. et al. The Sikkim flood of October 2023: Drivers, causes, and impacts of a multihazard cascade. *Science* **387**, eads2659 (2025).
6. Clague, J. J. & Evans, S. G. A review of catastrophic drainage of moraine-dammed lakes in British Columbia. *Quat. Sci. Rev.* **19**, 1763–1783 (2000).
7. Emmer, A. et al. 160 glacial lake outburst floods (GLOFs) across the Tropical Andes since the. *Glob. Planet. Change* **208**, 103722 (2022).
8. Anaconda, P. I., Mackintosh, A. & Norton, K. P. Hazardous processes and events from glacier and permafrost areas: lessons from the Chilean and Argentinean Andes. *Earth Surf. Proc. Land.* **40**, 2–21 (2015).
9. Wilson, R. et al. Glacial lakes of the Central and Patagonian Andes. *Glob. Planet. Change* **162**, 275–291 (2018).
10. Emmer, A. et al. Progress and challenges in glacial lake outburst flood research (2017–2021): a research community perspective. *Nat. Hazards Earth Syst. Sci.* **22**, 3041–3060 (2022).
11. Haeberli, W., Schaub, Y. & Huggel, C. Increasing risks related to landslides from degrading permafrost into new lakes in deglaciating mountain ranges. *Geomorphology* **293**, 405–417 (2017).
12. Ding, Y. et al. Increasing cryospheric hazards in a warming climate. *Earth Sci. Rev.* **213**, 103500 (2021).
13. Iles, C. E. et al. Strong regional trends in extreme weather over the next two decades under high-and low-emissions pathways. *Nat. Geosci.* **17**, 845–850 (2024).
14. Veh, G. et al. Trends, breaks, and biases in the frequency of reported glacier lake outburst floods. *Earths Future* **10**, e2021EF002426 (2022).
15. Carrivick, J. L. & Tweed, F. S. A global assessment of the societal impacts of glacier outburst floods. *Glob. Planet. Change* **144**, 1–16 (2016).
16. Harrison, S. et al. Climate change and the global pattern of moraine-dammed glacial lake outburst floods. *Cryosphere* **12**, 1195–1209 (2018).
17. Veh, G., Korup, O., von Specht, S., Roessner, S. & Walz, A. Unchanged frequency of moraine-dammed glacial lake outburst floods in the Himalaya. *Nat. Clim. Change* **9**, 379–383 (2019).
18. Beaulieu, C., Gallagher, C., Killick, R., Lund, R. & Shi, X. A recent surge in global warming is not detectable yet. *Commun. Earth Environ.* **5**, 576 (2024).
19. Shugar, D. H. et al. Rapid worldwide growth of glacial lakes since 1990. *Nat. Clim. Change* **10**, 939–945 (2020).
20. Zhang, T., Wang, W. & An, B. Heterogeneous changes in global glacial lakes under coupled climate warming and glacier thinning. *Commun. Earth Environ.* **5**, 374 (2024).
21. Zhang, T., Wang, W., An, B. & Wei, L. Enhanced glacial lake activity threatens numerous communities and infrastructure in the Third Pole. *Nat. Commun.* **14**, 8250 (2023).
22. Mergili, M. et al. How well can we simulate complex hydro-geomorphic process chains? The 2012 multi-lake outburst flood in the Santa Cruz Valley (Cordillera Blanca, Perú). *Earth Surf. Proc. Land* **43**, 1373–1389 (2018).
23. Maurer, J. M. et al. Seismic observations, numerical modeling, and geomorphic analysis of a glacier lake outburst flood in the Himalayas. *Sci. Adv.* **6**, eaba3645 (2020).
24. Sattar, A., Haritashya, U. K., Kargel, J. S. & Karki, A. Transition of a small Himalayan glacier lake outburst flood to a giant transborder flood and debris flow. *Sci. Rep.* **12**, 12421 (2022).
25. Carey, M., Huggel, C., Bury, J., Portocarrero, C. & Haeberli, W. An integrated socio-environmental framework for glacier hazard management and climate change adaptation: lessons from Lake 513, Cordillera Blanca, Peru. *Clim. Change* **112**, 733–767 (2012).
26. Wang, W., Zhang, T., Yao, T. & An, B. Monitoring and early warning system of Cirenmaco glacial lake in the central Himalayas. *Int. J. Disast. Risk Re.* **73**, 102914 (2022).
27. Emmer, A., Vilímek, V., Huggel, C., Klimeš, J. & Schaub, Y. Limits and challenges to compiling and developing a database of glacial lake outburst floods. *Landslides* **13**, 1579–1584 (2016).
28. Komori, J., Koike, T., Yamanokuchi, T. & Tshering, P. Glacial lake outburst events in the Bhutan Himalayas. *Glob. Environ. Res.* **16**, 59–70 (2012).
29. Veh, G., Korup, O., Roessner, S. & Walz, A. Detecting Himalayan glacial lake outburst floods from Landsat time series. *Remote Sens. Environ.* **207**, 84–97 (2018).
30. Colavitto, B. et al. A glacial lake outburst floods hazard assessment in the Patagonian Andes combining inventory data and case-studies. *Sci. Total Environ.* **916**, 169703 (2024).
31. Nie, Y. et al. An inventory of historical glacial lake outburst floods in the Himalayas based on remote sensing observations and geomorphological analysis. *Geomorphology* **308**, 91–106 (2018).
32. Lützwow, N., Veh, G. & Korup, O. A global database of historic glacier lake outburst floods. *Earth Syst. Sci. Data* **15**, 2983–3000 (2023).
33. Lliboutry, S., Pautre, A. & Schneider, B. Glaciological problems set by the control of dangerous lakes in Cordillera Blanca, Peru. *J. Glaciol.* **18**, 239–254 (1977).
34. Allen, S. K., Rastner, P., Arora, M., Huggel, C. & Stoffel, M. Lake outburst and debris flow disaster at Kedarnath, June 2013: hydro-meteorological triggering and topographic predisposition. *Landslides* **13**, 1479–1491 (2016).
35. Chen, N. et al. Small outbursts into big disasters: Earthquakes exacerbate climate-driven cascade processes of the glacial lakes failure in the Himalayas. *Geomorphology* **422**, 108539 (2023).
36. Sattar, A., Emmer, A., Lhazom, T., Rai, S. K. & Azam, M. F. Flood risk from small mountain lakes. *Commun. Earth Environ.* **6**, 785 (2025).
37. Emmer, A. et al. 70 years of lake evolution and glacial lake outburst floods in the Cordillera Blanca (Peru) and implications for the future. *Geomorphology* **365**, 107178 (2020).
38. Stuart-Smith, R. F., Roe, G. H., Li, S. & Allen, M. R. Increased outburst flood hazard from Lake Palcacocha due to human-induced glacier retreat. *Nat. Geosci.* **14**, 85–90 (2021).
39. Emmer, A. & Cochachin, A. The causes and mechanisms of moraine-dammed lake failures in the Cordillera Blanca, North American Cordillera, and Himalayas. *AUC Geogr.* **48**, 5–15 (2013).
40. Failletaz, J., Funk, M. & Vincent, C. Avalanching glacier instabilities: Review on processes and early warning perspectives. *Rev. Geophys.* **53**, 203–224 (2015).
41. Gilbert, A. et al. Mechanisms leading to the 2016 giant twin glacier collapses, Aru Range, Tibet. *Cryosphere* **12**, 2883–2900 (2018).
42. Fischer, L., Amann, F., Moore, J. R. & Huggel, C. Assessment of periglacial slope stability for the 1988 Tschierwa rock avalanche (Piz Morteratsch, Switzerland). *Eng. Geol.* **116**, 32–43 (2010).
43. Allen, S. K., Cox, S. C. & Owens, I. F. Rock avalanches and other landslides in the central Southern Alps of New Zealand: a regional study considering possible climate change impacts. *Landslides* **8**, 33–48 (2011).
44. Coe, J. A., Bessette-Kirton, E. K. & Geertsema, M. Increasing rock-avalanche size and mobility in Glacier Bay National Park and Preserve, Alaska detected from 1984 to 2016 Landsat imagery. *Landslides* **15**, 393–407 (2018).
45. Jacquemart, M. et al. Detecting the impact of climate change on alpine mass movements in observational records from the European Alps. *Earth Sci. Rev.* **258**, 104886 (2024).
46. Geertsema, M. et al. The 28 November 2020 landslide, tsunami, and outburst flood—A hazard cascade associated with rapid deglaciation at Elliot Creek, British Columbia, Canada. *Geophys. Res. Lett.* **49**, e2021GL096716 (2022).
47. Stoffel, M., Trappmann, D. G., Coullie, M. I., Cánovas, J. A. B. & Corona, C. Rockfall from an increasingly unstable mountain slope driven by climate warming. *Nat. Geosci.* **17**, 249–254 (2024).

48. Zhang, T., Wang, W., Shen, Z. & An, B. Increasing frequency and destructiveness of glacier-related slope failures under global warming. *Sci. Bull.* **69**, 30–33 (2024).
49. Hugonnet, R. et al. Accelerated global glacier mass loss in the early twenty-first century. *Nature* **592**, 726–731 (2021).
50. Dussaillant, I. et al. Annual mass change of the world's glaciers from 1976 to 2024 by temporal downscaling of satellite data with in situ observations. *Earth Syst. Sci. Data* **17**, 1977–2006 (2025).
51. Wang, X. et al. Glacial lake inventory of high-mountain Asia in 1990 and 2018 derived from Landsat images. *Earth Syst. Sci. Data* **12**, 2169–2182 (2020).
52. Ma, J., Song, C. & Wang, Y. Spatially and Temporally Resolved Monitoring of Glacial Lake Changes in Alps During the Recent Two Decades. *Front. Earth Sci.* **9**, 723386 (2021).
53. Wood, J. L. et al. Contemporary glacial lakes in the Peruvian Andes. *Glob. Planet. Change* **204**, 103574 (2021).
54. Veh, G. et al. Progressively smaller outbursts despite worldwide growth of glacier lakes. *Nat. Water* **3**, 3–13 (2025).
55. Rick, B., McGrath, D., Armstrong, W. & McCoy, S. W. Dam type and lake location characterize ice-marginal lake area change in Alaska and NW Canada between 1984 and 2019. *Cryosphere* **16**, 297–314 (2022).
56. Piroton, V. et al. Geomorphological processes and landforms in the Alpine Sulzenau Valley (Tyrol, Austria): Glacier retreat, glacial lake evolution and the 2017 glacial lake outburst flood. *Earth Surf. Proc. Land.* **49**, 4823–4841 (2024).
57. Carey, M. et al. Integrated approaches to adaptation and disaster risk reduction in dynamic socio-cryospheric systems. In *Snow and Ice-related Hazards, Risks, and Disasters*, 219–261. (Academic Press, 2015).
58. Emmer, A. Vanishing evidence? On the longevity of geomorphic GLOF diagnostic features in the Tropical Andes. *Geomorphology* **422**, 108552 (2023).
59. Corral, Á & González, Á Power law size distributions in geoscience revisited. *Earth Space Sci.* **6**, 673–697 (2019).
60. Li, L., Lan, H. & Wu, Y. How sample size can effect landslide size distribution. *Geoenviron. Disasters* **3**, 18 (2016).
61. Taylor, C., Robinson, T. R., Dunning, S., Rachel Carr, J. & Westoby, M. Glacial lake outburst floods threaten millions globally. *Nat. Commun.* **14**, 487 (2023).
62. IPCC, Intergovernmental Panel on Climate Change. *Managing the Risks of Extreme Events and Disasters to Advance Climate Change Adaptation*. A Special Report of Working Groups I and II of the Intergovernmental Panel on Climate Change (Cambridge University Press, New York, 2012).
63. Niggli, L. et al. *GLOF Risk Management Experiences and Options: A Global Overview* (Oxford Research Encyclopedias Natural Hazard Science, 2024).
64. Ribes, A., Qasmi, S. & Gillett, N. P. Making climate projections conditional on historical observations. *Sci. Adv.* **7**, eabc0671 (2021).
65. Esper, J., Torbenson, M. & Büntgen, U. 2023 summer warmth unparalleled over the past 2,000 years. *Nature* **631**, 1–2 (2024).
66. Rounce, D. R. et al. Global glacier change in the 21st century: every increase in temperature matters. *Science* **379**, 78–83 (2023).
67. Huss, M. et al. Toward mountains without permanent snow and ice. *Earths Future* **5**, 418–435 (2017).
68. Ahmed, R. Glacial lake outburst flood (GLOF) hazard and risk management strategies: a global overview. *Water Resour. Manag.* **39**, 1–16 (2025).
69. Zhang, G. et al. Characteristics and changes of glacial lakes and outburst floods. *Nat. Rev. Earth Environ.* **1**, 16 (2024).
70. Zaginaev, V. et al. Reconstruction of glacial lake outburst floods in northern Tien Shan: implications for hazard assessment. *Geomorphology* **269**, 75–84 (2016).
71. Medeu, A. R. et al. Moraine-dammed glacial lakes and threat of glacial debris flows in South-East Kazakhstan. *Earth Sci. Rev.* **229**, 103999 (2022).
72. Shrestha, F. et al. A comprehensive and version-controlled database of glacial lake outburst floods in High Mountain Asia. *Earth Syst. Sci. Data* **15**, 3941–3961 (2023).
73. Zheng, G. et al. Numerous unreported glacial lake outburst floods in the Third Pole revealed by high-resolution satellite data and geomorphological evidence. *Sci. Bull.* **66**, 1270–1273 (2021).
74. Wiczorek, I., Strzelecki, M. C., Stachnik, Ł, Yde, J. C. & Matceki, J. Post-Little Ice Age glacial lake evolution in Svalbard: inventory of lake changes and lake types. *J. Glaciol.* **69**, 1449–1465 (2023).
75. Mergili, M. & Schneider, J. F. Regional-scale analysis of lake outburst hazards in the southwestern Pamir, Tajikistan, based on remote sensing and GIS. *Nat. Hazards Earth Syst. Sci.* **11**, 1447–1462 (2011).
76. Wang, W. et al. A generic framework for glacial lake outburst flood investigation: a case study of Zalai Tsho, Southeast Tibet. *Catena* **234**, 107614 (2024).
77. Harris, I., Osborn, T. J., Jones, P. & Lister, D. Version 4 of the CRU TS monthly high-resolution gridded multivariate climate dataset. *Sci. Data* **7**, 109 (2020).
78. Wood, J. L. et al. Shaking up assumptions: earthquakes have rarely triggered Andean glacier lake outburst floods. *Geophys. Res. Lett.* **51**, e2023GL105578 (2024).
79. Cunningham, C. X., Williamson, G. J. & Bowman, D. M. Increasing frequency and intensity of the most extreme wildfires on Earth. *Nat. Ecol. Evol.* **8**, 1420–1425 (2024).
80. Zhang, T. Generalized additive model. *Zenodo* <https://doi.org/10.5281/zenodo.17694960> (2025).

## Acknowledgements

This study was supported by the National Key R&D Program of China (2024YFF0808603), the Second Tibetan Plateau Scientific Expedition and Research (STEP) Program (2024QZKK0500; 2024QZKK0400), and the National Natural Science Foundation of China (U23A2011).

## Author contributions

T.Z. analyzed data and wrote the draft of the manuscript. W.W., B.A. and T.Y. designed the study and edited the manuscript. I.K., S.J.C., P.I.A., and C.S.W. contributed to revise the GLOF inventory. S.L. linked climate change and GLOF activity together. All authors contributed to revise the manuscript.

## Competing interests

The authors declare no competing interests.

## Additional information

**Supplementary information** The online version contains supplementary material available at <https://doi.org/10.1038/s41467-025-67650-3>.

**Correspondence** and requests for materials should be addressed to Weicai Wang.

**Peer review information** *Nature Communications* thanks the anonymous reviewers for their contribution to the peer review of this work. A peer review file is available.

**Reprints and permissions information** is available at <http://www.nature.com/reprints>

**Publisher's note** Springer Nature remains neutral with regard to jurisdictional claims in published maps and institutional affiliations.

**Open Access** This article is licensed under a Creative Commons Attribution-NonCommercial-NoDerivatives 4.0 International License, which permits any non-commercial use, sharing, distribution and reproduction in any medium or format, as long as you give appropriate credit to the original author(s) and the source, provide a link to the Creative Commons licence, and indicate if you modified the licensed material. You do not have permission under this licence to share adapted material derived from this article or parts of it. The images or other third party material in this article are included in the article's Creative Commons licence, unless indicated otherwise in a credit line to the material. If material is not included in the article's Creative Commons licence and your intended use is not permitted by statutory regulation or exceeds the permitted use, you will need to obtain permission directly from the copyright holder. To view a copy of this licence, visit <http://creativecommons.org/licenses/by-nc-nd/4.0/>.

© The Author(s) 2025